Plant, Cell & Environment

WILEY

Plant, Cell & Environment

ORIGINAL ARTICLE

Switch From Soil to Plant Host Lifestyle Is Mediated by *rpoS* Mutations in Bacterial Endophyte

Wiam Alsharif[1] | Cristina Andrés-Barrao[1] | Sabiha Parween[1] | Abdulrahman Hashim[1] | Kirti Shekhawat[1] | Michael Abrouk[2] | Jian You Wang[2] | Ramona Marasco[2] | Simon G. Krattinger[2] | Daniele Daffonchio[2,3] | Salim Al-Babili[2] | Maged M. Saad[1] | Heribert Hirt[1,4]

[1]Darwin21 Desert Research Initiative, Biological and Environmental Sciences and Engineering Division (BESE), King Abdullah University of Science and Technology (KAUST), Thuwal, Saudi Arabia | [2]Biological and Environmental Sciences and Engineering Division (BESE), King Abdullah University of Science and Technology (KAUST), Thuwal, Saudi Arabia | [3]Department of Agriculture, Forestry and Food Sciences (DISAFA), University of Turin, Grugliasco, Italy | [4]Max Perutz Laboratories, University of Vienna, Vienna, Austria

Correspondence: Maged M. Saad (maged.saad@kaust.edu.sa) | Heribert Hirt (heribert.hirt@kaust.edu.sa)

Received: 24 January 2025 | **Revised:** 22 July 2025 | **Accepted:** 24 July 2025

Funding: This study was supported by KAUST grant BAS/1/1062-01-01 to H.H. D.D. acknowledges the support of KAUST for the Biolog system analysis through the baseline funding.

Keywords: bacterial endophyte | bacterial evolution | nutrient adaptation | plant-microbe interaction | rpoS sigma factor | selective pressure

ABSTRACT

Phenotypic switching in bacteria is a well-established evolutionary strategy that enhances fitness in response to changing environmental conditions. Here, we hypothesised that the observed phenotypic transition of the soil-dwelling *Enterobacter* sp. SA187—from yellow- to white-pigmented colonies upon plant root colonisation—reflects such an adaptive mechanism. This phenotypic switching is not host-specific but occurs consistently during the colonisation of various plant species. Through genome re-sequencing of switcher white colonies, we identified recurrent loss-of-function mutations in the *rpoS* gene compared to the yellow ancestral strain. Functional validation confirmed that mutations in *rpoS* are both necessary and sufficient to trigger the phenotypic switch, leading to widespread transcriptional changes affecting traits involved in plant colonisation, including motility, biofilm formation, metabolism, and growth rate. Metabolic profiling further revealed that the SA187 switcher variant exhibited enhanced fitness in conditions mimicking the acidic, sucrose-rich apoplastic environment of plant tissues, supporting the idea that this phenotypic switch represents a specific adaptation to the endophytic niche. Overall, our findings highlight the pivotal role of *rpoS*-mediated regulation in facilitating the transition of SA187 from a free-living to endophytic lifestyle and provide mechanistic insights into how bacterial symbionts dynamically adapt through phenotypic switching during host colonisation.

1 | Introduction

Similar to the gut microflora of animals, plants have established beneficial interactions with a wide range of bacterial species. Throughout evolution, these beneficial bacteria likely helped plants cope with the new and stressful conditions associated with life on land (Hirt 2020). Many plant-growth-promoting (PGP) microorganisms colonise plant roots to exert their beneficial effects. While epiphytic strains colonise root surfaces, endophytic strains inhabit the internal tissues of the plant host (Bisseling et al. 2009; Liu et al. 2017). Although PGP microorganisms often exhibit relatively broad host ranges, soil properties and environmental conditions also play key roles in shaping these beneficial plant-microbial interactions (Berg and Smalla 2009; Drogue et al. 2012).

Rhizobacteria are initially recruited from the soil to the rhizosphere—the critical interface between soil and plant roots,

where a delicate trade-off between nutrition exchange and defence takes place. These microorganisms are attracted by root exudates, which consist primarily of organic acids, vitamins, simple sugars and polysaccharides. These compounds, actively released by plant roots, influence the physico-chemical properties of the surrounding soil (Bais et al. 2006; Haichar et al. 2014; Massalha et al. 2017), thereby attracting different microorganisms (Haichar et al. 2014). Depending on soil characteristics and environmental conditions (Rudrappa et al. 2008; Yuan et al. 2018), plants can modulate the composition of their root exudates and thus shape the rhizosphere microbial community in a dynamic and responsive manner (Ankati and Podile 2019; Haichar et al. 2008; Marasco et al. 2022; Massalha et al. 2017; Reinhold-Hurek et al. 2015).

Soils harbour extremely complex microbial communities that include a wide diversity of bacterial taxa (Philippot et al. 2024). Among them, competent bacterial strains can establish interactions with plants, initiating the colonisation of root tissues. This process typically begins with the attachment of bacterial cells to root epidermis, facilitated by the production of extracellular polysaccharides or adhesive proteins (Wheatley and Poole 2018). Following this attachment, bacterial cells can exploit natural entry points such as sites of lateral root emergence, root hairs, or wounds to access the plant interior (Hardoim et al. 2015). Once inside the plant tissues, microorganisms encounter an environment that differs markedly from the surrounding soil. In particular, the intercellular spaces of plant tissues (i.e., the apoplast) are characterised by variable osmotic and water-potential dynamics, nutrient specificity (i.e., simple sugars like sucrose and organic acids), and a more acidic pH. These conditions contrast sharply with the typically dry, nutrient-poor and alkaline environments of desert soils (Eida et al. 2018; Hirt 2020), so it is plausible to expect that such bacteria entering the root tissues must rapidly remodel their physiology and metabolic pathways to exploit the apoplast's resources and maintain homoeostasis.

To investigate how bacteria adapt during their transition from a free-living lifestyle in soil to an endophytic lifestyle within a plant host, we studied the colonisation process of Arabidopsis by the beneficial bacterium *Enterobacter* sp. SA187. This yellow-pigmented strain was originally isolated from *Indigofera argentea*, a leguminous plant native to semi-desert regions of the Arabian Peninsula (Andrés Barrao et al. 2017). In addition to its natural host, SA187 can also colonise Arabidopsis, alfalfa, and wheat, where it has been shown to confer tolerance to abiotic stress (de Zélicourt et al. 2018; Shekhawat et al. 2021; Shekhawat et al. 2024). The SA187 strain preferentially colonises primary roots by producing pectinases and proteases that allow it to penetrate the root epidermis, particularly in the elongation zone. This process enables this bacterium to enter and colonise the root apoplastic spaces throughout root tissues (Synek et al. 2021). During re-isolation from inoculated plant tissues, we consistently observed that formerly yellow-pigmented SA187 (SA187Y) colonies gave rise to white-pigmented variants (SA187W) (Andrés Barrao et al. 2017). We hypothesise that this reproducible phenotypic switch (Supporting Figure S1) reflects underlying bacterial adaptive mechanisms evolved to cope with the starkly different selective pressure of the endophytic niche. As rooted in several related biological concepts and theories (among others, bet-hedging and phenotypic plasticity), organisms in fluctuating environments benefit from regulatory circuits that enable rapid phenotype changes in response to new conditions. In the case of endophytes, the plant's intracellular milieu imposes a suite of challenges, including acidic pH, sucrose-rich but micronutrient-scarce medium, oxidative bursts, and immune surveillance that are absent in the soil. Thus, it is plausible that bacteria capable of colonising root tissues from the surrounding soil, such as *Enterobacter* sp. SA187, may adapt to the new conditions by diversifying in subpopulations/phenotypes to maximise fitness and colonisation efficiency. For instance, phenotypic switching, via phenotypic plasticity or bet-hedging, allows subpopulations to diversify into motile, biofilm-forming, or stress-tolerant morphologies, balancing growth and survival. Mechanistically, such switches often involve regulatory changes at the level of gene networks, including operons and regulons (Crombach and Hogeweg 2008; Krell et al. 2010). By incorporating such genetic or epigenetic switches, microorganisms can tune their phenotypic mix—balancing growth versus stress-tolerance—in a process in which subpopulations adopt discrete physiological states, thereby generating phenotypic heterogeneity and specialised traits (Henderson et al. 1999; van der Woude and Bäumler 2004). Phenotypic heterogeneity may also arise stochastically within isogenic populations, enabling rapid adaptation to fluctuating environmental conditions (for review, see Morawska et al. 2022).

To test our hypothesis and elucidate the molecular and physiological mechanisms underlying the phenotypic switch from SA187Y to SA187W, we implemented an integrative workflow combining comparative genomics, transcriptomic profiling, and targeted mutagenesis. In addition, we performed phenotypic characterisation and plant-interaction assays to evaluate how these changes influence the phenotypic plasticity of SA187 and its ability to establish a successful endophytic relationship with its host, as well as to promote plant tolerance to abiotic stress, such as salinity. Our results demonstrate that the transition of *Enterobacter* sp. SA187 from the free-living soil lifestyle to the endophytic lifestyle *in planta* is consistently mediated by genetic modifications in the *rpoS* gene. These modifications adapt the physiology and metabolism of SA187 to the specific conditions of the plant root apoplast, as a result of its endophytic colonisation.

2 | Materials and Methods

2.1 | Preparation of *Enterobacter* sp. S187 Bacterial Cultures

Bacterial cultures of *Enterobacter* sp. SA187 strain variants (SA187Y and SA187W) were routinely revived from glycerol stocks stored at −80°C. For this, bacteria were streaked onto lysogeny broth (LB, Luria-Bertani, Invitrogen) agar plates and incubated at 28°C for 24 h to obtain isolated colonies. A single colony was then picked and inoculated into 5 mL of LB liquid medium and incubated overnight at 28°C with shaking at 220 rpm to obtain a pre-culture. Based on the specific experimental requirements described below, this pre-culture was subsequently used to prepare fresh cultures in different ways.

Unless otherwise specified, 100 μL of the overnight pre-culture was used to inoculate 25 mL of LB medium in triplicate. Cultures were incubated at 28°C with shaking at 220 rpm until the desired growth stage was reached.

2.2 | Preparation of Media and Experimental Setup for Arabidopsis Growth

Half-strength Murashige-Skoog Basal Salt broth (Sigma, Germany; ½ MS, pH 5.8) was prepared and cooled to 37°C-40°C. For inoculation, 50 mL of the ½ MS media was supplemented with 100 μL of a bacterial suspension containing 10^7 cells, corresponding to an optical density at 600 nm (OD_{600}) of 0.21. As control, 50 mL ½ MS medium was inoculated with 100 μL of liquid LB without bacteria. All plates were left to solidify before further use. Arabidopsis seeds were surface sterilised by 10 min shaking in 1 mL of 70% ethanol added with 0.05% sodium dodecyl sulphate (SDS) and washed 2-3 times in 1 mL of Milli-Q water. Sterilised seeds were sown on the inoculated ½ MS plates and control plates. Seeds were incubated for 2 days at 4°C in the dark to mimic seed stratification, and then germination was allowed on vertical plates in Percival incubators (22°C, 16 h light cycle) for 5 days. After this, seedlings were transferred to new plates under normal conditions (½ MS agar plates) or salt stress (½ MS agar plates supplemented with 100 mM NaCl). This setup was used to assess bacterial colonisation and plant-growth-promoting effects; the number of replicates and independent experiments conducted was reported for each assay in the related paragraphs.

2.3 | Assessment of Bacterial Colonisation in Arabidopsis

To quantify the number of viable bacteria colonising plant tissues, colony-forming units (CFU) per milligram of sample were determined at specific time points: daily from day 1 to day 10, and then every 2 days until day 18. Arabidopsis and growth media were prepared as described above. Time point T0 refers to 5-day-old seedlings transferred onto different conditions, that is, ½ MS and ½ MS supplemented with 100 mM NaCl. Final plates contained six seedlings each, and three plates were prepared for each treatment (i.e., bacteria tested vs control) and condition (i.e., normal vs salinity). The experiment was repeated three times. At each measurement, one seedling was collected from each plate (three seedlings total) for CFU quantification. Bacteria were isolated without any surface sterilisation of the plants. The collected plants were transferred into 2 mL sterile tubes containing metal beads and weighed. Samples were homogenised by using the TissueLyser II (QIAGEN). Then, 500 μL of 100 mM $MgCl_2$ supplemented with 0.02% Silwet L-77 was added, and samples were homogenised again. Homogenised plant samples were serially diluted (1:10) in 100 mM $MgCl_2$ supplemented with 0.02% Silwet L-77, and up to 10^6-fold dilution was reached. Aliquots of 10 μL from each dilution were plated onto LB agar medium plates and incubated at 28°C. Colonies were counted the following day, distinguishing between yellow- and white-pigmented types, and CFU counts were expressed per milligram of plant tissue.

2.4 | Biochemical Characterisation of SA187 Variants

The strain variants SA187Y and SA187Y were grown overnight in LB following the standard procedure described above. The cultures were subsequently used to characterise their metabolic, physiological and morphological traits under controlled laboratory conditions.

2.4.1 | Growth Curves

To assess the impact of phenotypic switch (i.e., from yellow- to white-pigmented colonies) on in vitro bacterial fitness, the growth dynamics of SA187Y and SA187W were monitored over 4 days. Freshly inoculated cultures were incubated in LB medium, and OD_{600} was measured manually. Measurements were recorded every hour during the first 12 h of growth, every 3 h thereafter until the onset of the stationary phase, and subsequently every 6 h.

2.4.2 | Co-culture of SA187Y and SA187W

To assess competitive growth between SA187Y and SA187W, 100 μL of each pre-culture was adjusted to an OD_{600} of 0.2 and further co-incubated in LB medium. Samples were collected at 8 and 24 h, and CFUs were determined by serial dilution and plating, distinguishing colonies based on pigmentation.

2.4.3 | Transfer of SA187Y Colonies to Different Media

SA187 colonies from LB medium were picked and streaked onto LB medium supplemented with 20% sucrose. Subsequently, the SA187W switch colonies obtained from exposure to sucrose were picked and transferred back onto standard LB medium.

2.4.4 | Biofilm Assays

Bacterial strains were grown overnight in LB broth at 28°C with shaking at 220 rpm. The following morning, fresh cultures were prepared by inoculating 5 mL of LB medium with 10 μL of the overnight culture and incubating for three to 4 h until reaching the exponential phase. Then, 10 μL of the refreshed cultures was spotted onto Congo Red medium (1% tryptone, 1% agar, 20 μg/mL Congo Red, and 10 μg/mL Coomassie brilliant blue G250). Plates were incubated at 28°C for up to 7 days to assess colony morphology and pigmentation.

2.4.5 | Motility Assays

Motility assays were performed by spot-inoculating 10 μL of 10^7 CFU/mL culture onto LB plates containing 0.3% agar for swimming motility and 0.6% agar for sliding motility. The plates were dried before use to ensure optimal surface moisture. Inoculated plates were incubated at 28°C for 2 days. Bacterial

migration from the colony's centre was assessed by measuring the radius of colony expansion across the agar surface.

2.4.6 | Catalase Activity Assays

Bacterial strains were grown overnight on LB agar medium at 28°C for 24 h. A drop of 30% (wt/wt) hydrogen peroxide solution (Sigma-Aldrich) was placed on a microscopic glass slide, and a loop of bacterial cells was immersed and gently streaked into the solution. The formation of bubbles indicated a positive catalase activity. All experiments were performed independently three times for each bacterial variant, with three replicates per experiment.

2.5 | Scanning Electron Microscopy of Ancestral and Switcher Variants of SA187

SA187Y and SA187W were grown in LB medium until log phase before transfer to track-etched polycarbonate filter membranes. Then, samples were fixed in glutaraldehyde 2.5% in 0.1 M cacodylate buffer (pH 7.3) overnight at 4°C. Samples were then washed three times in 0.1 M cacodylate for 15 min each, postfixed in 1% osmium tetroxide in 0.1 M cacodylate for 1 h in darkness, washed three times in Milli-Q water for 15 min each, and dehydrated through a gradient of ethanol: 30%, 50%, 70%, 90% and 100%, for 15 min each. Samples were then further dehydrated two times in 100% ethanol for 15 min each and dried in a Point Dryer EM CPD300 (Leica, Saudi Arabia). Dried samples were mounted on a stainless stub, coated with Pt/Pd in a K575 Sputter Coater (Emitech, UAE), and observed in a Teneo VS Microscope (ThermoFisher, USA). To assess bacterial cell length, two independent biological replicates were prepared for each strain, SA187Y and SA187W, each originating from a separate colony. For each of them, 14–16 microscopy slides were analysed. A total of 100–120 microscopic fields were imaged and measured, yielding approximately 950 individual cell measurements per strain. Bacterial lengths were quantified using a Teneo VS Microscope (ThermoFisher, USA), Imaging and Characterisation Core Lab (IAC), KAUST. Statistical comparisons between the two strains were performed using a two-tailed unpaired *t*-test.

2.6 | Metabolic Characterisation of SA187Y and SA187W Variants

Biolog Phenotype MicroArray (PMs) technology (Biolog Inc., Hayward, CA, USA) was applied to assess the metabolic profiles of the SA187Y and SA187W variants. Fresh LB agar plates were prepared from glycerol stocks and incubated overnight following the standard procedures described above. Cells were collected from the plate surface using sterile cotton swabs and suspended in physiological saline solution (9 g/L NaCl). Cell density was adjusted to 85% transmittance on a Biolog turbidimeter. According to the manufacturer's instructions, a 1:200 dilution of the bacterial suspension was prepared in the appropriate inoculation fluids: (i) IF-0 for PM1 and PM2 (carbon utilisation) and (ii) LB medium for PM9 (osmotic/ionic response) and PM10 (pH response). Tetrazolium-based redox dye Biolog Redox Dye A (1×) was added to the inoculation fluids to monitor and quantify cellular respiration (NADH production) as an indicator of metabolic activity. Inoculation fluids were dispensed into PM plates (120 μL per well). Plates were incubated at 28°C in the OmniLog instrument for 72 h, and the colour development was monitored automatically every 25 min for changes. The collected data were analysed using Kinetic and Parametric software (Biolog), which generated time course curves of tetrazolium reduction. The area under the kinetic curve of dye formation was calculated and compared to assess differences in metabolic activity between the two variants. All plates used in the experiments were prepared in duplicate for each bacterial strain variant.

2.7 | Bacterial DNA Extraction and MiSeq Genome Sequencing of SA187 Variants

A total of 100 yellow-pigmented (SA187Y) and 100 white-pigmented (SA187W) colonies were re-isolated from colonised Arabidopsis plants following the inoculation and incubation conditions previously described. Genomic DNA was extracted from individual colonies using the GenElute Gel Extraction Kit (Sigma Aldrich, USA), following the manufacturer's recommendations. For downstream analyses, genomic DNA from the SA187Y and SA187W colonies was pooled into composite samples, with each pool comprising DNA from 10 individual colonies. In total, 20 pooled samples were generated, 10 for SA187Y and 10 for SA187W. DNA purity and concentration of the pool were further assessed using a NanoDrop-6000 spectrophotometer and the Qubit 2.0 Fluorometer with the DNA BR assay kit (Invitrogen). TruSeq DNA Nano libraries were prepared following the manufacturer's instructions and quality-checked by Bioanalyzer (Agilent Technologies) and Qubit. Libraries were pooled equimolarly, and the library was checked again for size distribution and the presence of unwanted artifacts using the Bioanalyzer. Library quantification was performed with the KAPA SYBR FAST Universal qPCR kit with Illumina Primer Premix (Kapa Biosystems Ltd.). A final concentration of 12 pM of the pool supplemented with 1% PhiX control was sequenced on the MiSeq Illumina platform using the 2 × 300 bp MiSeq reagent kit V3 at the Bioscience Core Lab (BCL) in KAUST.

2.8 | Raw Reads Filtering, Alignment, and Variant Calling

The raw sequencing reads obtained from the 10 SA187Y pools and 10 SA187W pools were first analysed with the fastqQC tool v0.11.7 (Thrash et al. 2018). Low-quality reads were filtered with Trimmomatic-v0.38 (Bolger et al. 2014) using the following criteria: LEADING:20; TRAILING:20; SLIDINGWINDOW:5:20 and MINLEN:50. Filtered paired-end reads were then individually aligned against the *Enterobacter* sp. SA187 reference genome (Andres-Barrao et al. 2017) using BWA-MEM (v0.7.17-r1188) (Li and Durbin 2010). The resulting alignments were sorted and indexed using SAMtools v1.6 (Li et al. 2009). Alignment metrics, including summary statistics, base quality score, and insert size distribution, were collected. Duplicated reads were marked, and read groups were assigned using Picard tools (http://broadinstitute.github.io/

picard/). Variant calling was performed with GATK v3.8 (McKenna et al. 2010) using the HaplotypeCaller algorithm with the –emitRefConfidence option to identify single nucleotide polymorphisms (SNPs) and insertion/deletion (INDELs), followed by a joint genotyping step performed by GenotypeGVCFs. To obtain high-confidence variants, SNPs and INDELs were filtered using the VariantFiltration function of GATK with the following criteria: QD < 2.0; FS > 60.0; MQ < 40.0; MQRankSum < − 12.5; ReadPosRankSum < − 8.0 and SOR > 4.0.

2.9 | Bacterial Total RNA Extraction, RNA-Seq and Bioinformatics Analysis

Total RNA was extracted from three cultures of SA187Y and SA187W grown in liquid medium at 6 and 18 h. The RNA extraction was performed using the RiboPure Bacteria kit (Ambion) following the manufacturer's instructions, with modifications described in (Andrés-Barrao et al. 2021). RNA concentration was measured using a Qubit 2.0 Fluorometer with the RNA BR assay kit (Invitrogen), and RNA integrity was assessed with a 2100 Bioanalyzer and the RNA 6000 Nano assay (Agilent Technologies). RNA libraries were prepared and sequenced by Novogene Bioinformatics Technology Co. Ltd. (Beijing, China) using the NovaSeq. 6000 PE150 platform (Illumina). Libraries were quantified by Qubit fluorometry and qPCR, and fragment size distribution was verified via Bioanalyzer. Quantified libraries were pooled and sequenced on Illumina platforms, following standard cluster generation and sequencing protocols, producing paired-end reads.

Raw FASTQ reads were quality-checked and pre-processed through fastp. Reads containing adaptor sequences, poly-N regions, or low-quality bases were trimmed to generate clean data. At the same time, Q20, Q30, and GC content metrics were calculated to ensure high-quality data for downstream analyses. FeatureCounts was used to count the number of reads mapped to each gene. Gene expression was quantified as Fragments Per Kilobase of transcript per Million mapped reads (FPKM) for each gene, considering gene length and sequence depth (Trapnell et al. 2010). Differential gene expression analysis was performed using the DESeq. 2 R package, which models count data based on the negative binomial distribution. The resulting *p*-values were adjusted for multiple testing using the Benjamini and Hochberg correction. Differentially expressed genes (DEGs) were identified using thresholds of adjusted *p*-value ≤ 0.05 and fold change ≥ 1.6. Gene Ontology (GO) annotation and functional enrichment analyses were conducted using the Integrated Data warehouse of Microbial Genomes from KSA deserts (INDIGO-Desert). DEG visualisation was performed in MeV v4.9.0 (TM4 platform, https://sourceforge.net/projects/mev-tm4/files/mev-tm4/MeV%204.9.0/) using Pearson correlation method. RNAseq data have been deposited in the NCBI Gene Expression Omnibus (GEO) database under the accession number GSE277260.

2.10 | Bacterial RNA-Seq Validation by qRT-PCR

To validate the results obtained from the bacterial RNA-Seq experiments, qRT-PCR was performed using primers targeting key genes involved in carotenoid biosynthesis. Specifically, primers were designed using the Primer-Blast online tool provided by the National Centre for Biotechnology Information (NCBI) (https://www.ncbi.nlm.nih.gov/tools/primer-blast/) on the following genes: *crtE* (geranylgeranyl diphosphate synthase), *idi* (isopentenyl-diphosphate delta-isomerase), *crtX* (zeaxanthin glucosyltransferase), *crtY* (lycopene beta cyclase), *crtB* (phytoene synthase) and *crtZ* (beta-carotene 3-hydroxylase). The translation initiation factor IF-2 (*infB*) was used as a reference gene (de Zélicourt et al. 2018). The cDNAs used as templates for qRT-PCR were synthesised with SuperScript III Reverse Transcriptase (Invitrogen) and oligo(dT) primers, following the manufacturer's recommendations. qRT-PCR reactions were carried out in a CFX96 Touch Real-Time PCR Detection System (Bio-Rad) under the following cycling conditions: an initial denaturation at 95°C for 10 min, followed by 40 cycles of denaturation at 95°C for 10 s and annealing/extension at 60°C for 40 s. A dissociation step (melting curve analysis) was included at the end of the run to validate the specificity of PCR products. All reactions were performed in triplicate. Relative gene expression levels were calculated using the $\Delta\Delta C_T$ method. Relative gene expression was compared separately for each gene between the two bacterial strains using an unpaired two-tailed Student's *t*-test in GraphPad Prism v10. The significance was set at $p < 0.05$.

2.11 | Quantification of Carotenoids in SA187 Strain Variants

Overnight cultures of SA187Y and SA187W were grown in LB medium at 28°C until reaching the stationary phase. Three biological replicates were prepared for each variant, and three samples were collected from each. Bacterial cells were collected by centrifugation at 5000 rpm for 12 min at 4°C, and the resulting pellets were washed twice with $MgSO_4$ to remove residual media. After washing, pellets were stored at −80°C until carotenoid extraction. Carotenoid extraction was performed following the procedure (Mi et al. 2018). UHPLC Ultimate 3000 system (Thermo Fisher Scientific, Waltham, MA, USA) equipped with a UV detector and autosampler was used for carotenoids analysis and quantification. The LC separation of carotenoids was performed with a gradient from 30% A to 100% A (A, methanol: tert-butylmethyl ether [1:1, vol/vol]; B, methanol: water: tert-butylmethyl ether [6:3:1, vol/vol/vol]) in 19 min, maintaining 100% A for 5 min, decreasing 100% A to 70% A in 1 min and washing of 5 min with 70%.

2.12 | Preparation of Competent Cells of *Enterobacter* sp. SA187

SA187 ancestral strain was grown on LB medium supplemented with 2.5% agar and incubated overnight at 28°C. A single colony was then used to inoculate a 40 mL LB broth and incubated for 16 h at 28°C with shaking at 220 rpm. The next day, 100 μL of the cultured bacterium was added to 40 mL liquid broth in a 250 mL flask and incubated at 28°C with shaking at 220 rpm until the culture reached an OD_{600} of 0.4. The cells were centrifuged, washed, and suspended in ice-cold glycerol 10%. They were then aliquoted and stored at −80°C in a 20% glycerol LB solution.

2.13 | Generating and Mapping the Tn5 Transposon Mutant Library of the *Enterobacter* sp. SA187

Competent cells and Tn5 DNA were thawed on ice from −80°C. Then, 0.5 μL of either lucigen-EZ-Tn5 or epicentre-EZ-Tn5 <R6Kγori/KAN-2> transposon material was added to 100 μL of competent cells and electroporated. After adding 900 μL of SOC media and mixing, the electroporated cells were incubated for 2 h at 28°C with shaking at 220 rpm. Next, 100 μL of incubated cells were spread on LB agar plates with 50 μg/mL kanamycin. The remaining 900 μL of cells were centrifuged, resuspended with 150 μL of H_2O, and spread on LB agar plates with 50 μg/mL kanamycin. These plates were incubated at 28°C for 24 h. Surviving yellow and/or white colonies were picked and suspended in 96-well plates with liquid LB and kanamycin. The plates were incubated at 28°C with shaking at 220 rpm for 16–24 h. The next morning, glycerol LB broth was added to the culture of mutants and stored at −80°C for further testing.

2.14 | Amplification of the Transposon Insertions in SA187 Variants, Purification of PCR Products, and Sequencing

Ten of the white colonies picked were used to confirm the insertion of Tn5 in the SA187 genome and evaluate its position. A PCR was performed on the bacterial genomic DNA. The primers provided in EZ-Tn5 are designed to read in the opposite direction of the inserted transposon material: KAN-2 FP-1 forward primer 5′-ACCTA CAACAAAGCTCTCATCAACC-3′ and KAN-2 RP-1 reverse primer 5′-GCAATGTAACATCAGAGATTTTGAG-3′. The amplification was carried out in a 25 μL reaction using 12 μL PCR Master Mix 2X (PROMEGA), 1.5 μL of forward and reverse primers (10 μM), 1 μL template DNA, and 9 μL nuclease-free water (PROMEGA). Amplification of both genes was performed in a C1000 Touch Thermo Cycler (Bio-Rad) with temperature and cycling conditions as follows: one denaturation cycle at 95°C for 5 min, followed by 30 cycles of denaturation at 95°C for 30 s, primer annealing at 60°C for 30 s, and elongation at 72°C for 5 min, finishing with 5 min incubation at 72°C. 5 μL of the PCR products were visualised on a 0.8% agarose gel prepared in 1 × TAE buffer. 22.5 μL of 10,000 × Syber safe DNA gel stain (Invitrogen) was added before pouring the gel. 6 × DNA gel-loading dye was used, and 1 kb Plus DNA Ladder (Thermo Scientific, GeneRuler) was used as a size marker, and the gel was run at 100 V. The DNA samples were visualised with the ChemiDoc MP Imaging System (Bio-Rad). Amplified PCR products were cleaned using ExoSAP-IT PCR Product Cleanup Reagent (Affymetrix), which enzymatically purifies the PCR products by hydrolysing the excess primers and nucleotides. 10 μL of the PCR product was mixed with 4 μL of ExoSAPIT reagent for a combined 14 μL reaction volume. The sample was incubated at 37°C for 15 min to degrade the remaining primers and nucleotides. Then it was incubated at 80°C for 15 min to inactivate ExoSAP-IT reagent. Then the purified PCR product was sent for DNA sequencing. The location of the transposon insertion was determined by direct Sanger sequencing at BCL (KAUST) using DNA extracted from the ten SA187 white clones. Sequencing was performed using the previously described EZ-Tn5 primers.

2.15 | Promotion of Arabidopsis Growth Mediated by the SA187 Strain Variants

Arabidopsis seeds and plates were prepared as previously described to evaluate the bacterial treatment's effect on plant growth. After incubation with bacterial strain variants SA187Y (ancestral), SA187W (switcher reisolated from Arabidopsis), SA187Ω*rpo*S (i.e., white-pigmented mutant generated by mutation of the *rpoS* gene), and SA187Ω*idi* (i.e., white-pigmented mutant generated by mutation of the *idi* gene), plantlets were transferred to ½ MS and ½ MS + 100 mM NaCl. Plates contained 6 seedlings each, and 2 plates were prepared for each treatment (i.e., bacteria tested vs control) and condition (i.e., normal vs salt). The experiment was repeated three times. Eight days after plant transfer, the plates were scanned, and the images were used to measure the principal root length using Image J software. The number of lateral roots was counted on day 8 for plants grown under ½ MS conditions and on day 12 for those grown under ½ MS supplemented with 100 mM NaCl. Lateral root density was then determined as the number of lateral roots per root length. Aerial fresh weight, root fresh weight, and total fresh weight were measured at the end of the experiment. Statistical analyses were performed in R (v4.2.0) using the lme4 package by fitting linear mixed-effects models (lmer) with Treatment as a fixed effect and "Experiment" and "Plate" factors as random intercepts to account for pseudoreplication.

2.16 | Effect of SA187 Strain Variants on Rice Growth

Seeds of rice *Oryza sativa* L. (cv. Nipponbare) were surface sterilised by soaking in 70% ethanol for 1–2 min with 2–3 manual washes. This was followed by treatment with 50% commercial bleach for 10 min, then rinsed thoroughly 2–3 times with sterile distilled water to remove residual bleach. Sterilised seeds were sown on the ½ MS plates inoculated with 10^7 cells of bacterial culture from SA187Y, SA187W, and SA187Ω*idi*; plates without bacterial inoculum were used as controls. Seeds were incubated for 3 days at 30°C in the dark. After dark incubation, plates were transferred to a growth chamber under light conditions for 5 days (28°C, 12 h light/12 h dark cycle, 60%–70% humidity). Seedlings were transferred to 50 mL tubes containing Hoagland's nutrient solution (full-strength), adjusted to pH 5.8. Rice seedlings were grown hydroponically and subjected to a progressive salt stress treatment over 5 weeks. During the second week, seedlings were transferred to a larger 5-liter hydroponic system to allow enhanced root and shoot development. Salt stress was applied gradually through the nutrient solution, with no salt added during the first week, followed by 25 mM NaCl in the second week, 50 mM in the third week, 75 mM in the fourth week, and 100 mM in the fifth week. Seedlings grown under the same conditions without salt treatment served as controls. The nutrient solution was refreshed twice per week during the first 2 weeks to maintain optimal nutrient availability, and once per week for the remainder of the experiment. At the end of the experiment, the number of tillers, shoot dry weight, and root dry weight were measured. Statistical analysis was performed using one-way ANOVA followed by Tukey's multiple comparisons test in GraphPad Prism v10 to assess

differences across treatments for each condition (i.e., normal and salt stress); significance was set at $p < 0.05$. Six individual plants grown in the same hydroponic box were analysed for each treatment. The experiment was conducted once.

3 | Results

3.1 | Phenotypic Switching of *Enterobacter* sp. SA187 Occurs Upon Plant Colonisation

Enterobacter sp SA187 typically forms characteristic yellow colonies (SA187Y) (Andrés Barrao et al. 2017). However, upon re-isolation from colonised Arabidopsis plants, a substantial number of white-pigmented colonies (SA187W) were consistently observed alongside yellow ones (Supporting information Figure S1A). Genotyping ruled out contamination and confirmed that both colony types belong to SA187, indicating a phenotypic switch within the same strain (Andrés Barrao et al. 2017), likely triggered by the internal conditions of plant tissue. The SA187W variant was also systematically re-isolated after colonisation of the original host (*I. argentea*), as well as other plants such as wheat and rice (Supporting information Figure S1B–D), demonstrating that the occurrence of phenotypic switchers is not host-specific. Notably, SA187W colonies re-isolated from plants did not revert to yellow pigmentation when propagated under standard laboratory conditions on LB medium, suggesting that the phenotypic switch is associated with stable genetic changes.

3.2 | Colonisation and Phenotypic Switch Dynamics of SA187 Under Normal and Salt Stress Conditions

To investigate the temporal dynamics of bacterial colonisation and phenotypic switching, 5-day-old Arabidopsis plantlets pre-colonised with SA187 yellow-pigmented ancestor (SA187Y) were transferred to bacteria-free ½ MS plates and incubated under normal conditions and salt stress (100 mM of NaCl) for a period of 18 days. Under normal conditions, the colonisation rate reached a peak of approximately 10^6 CFU/mg between T2 (2 days) and T9 (9 days) before gradually declining (Figure 1A, see red dotted line as reference). A similar pattern was observed under salt stress, although the decline was less pronounced (Figure 1B), which may indicate a more stable colonisation pattern when the host is exposed to challenging environmental conditions, here tested as salinity. However, considering colony pigmentation, white-pigmented switchers (SA187W) began to emerge 4 days after transfer under normal conditions (T4, Figure 1C), and as early as 24 h after salt stress exposure (T1, Figure 1D). Under normal conditions, the proportion of SA187W colonies gradually increased over time, resulting in a mixed population of approximately 35% SA187Y and 65% SA187W by day 18 (Figure 1C). In contrast, under salt stress, the population predominantly comprised SA187W (86%) by day 18 (Figure 1D). These results suggest that environmental stress, like salinity, can trigger phenotypic switching in SA187, accelerating the phenotypic transition from yellow to white pigmentation.

3.3 | SA187 Switchers Have Distinct Growth Properties, Morphology, and Physiology

To determine whether SA187W switchers present different growth patterns compared to the ancestral SA187Y strain, we analysed the growth curves of both variants in LB medium. SA187Y consistently reached higher optical densities than the switcher (Supporting information Figure S2A). This difference was already evident during the logarithmic phase and became more pronounced at 12 h when SA187W had entered the stationary phase, while SA187Y continued its exponential growth until 24 h. Yet, to assess whether SA187Y and SA187W compete for nutrients, we examined their growth patterns in coculture, starting from equal cell densities. At both 8 and 24 h, SA187W consistently exhibited lower CFU counts compared to SA187Y (Supporting information Figure S1E,F, respectively). The reduced growth of SA187W in nutrient-rich LB medium likely reflects intrinsic physiological differences in this switcher variant, as well as may also suggest that SA187W has altered or more specific nutrient requirements, potentially acquired/selected as an adaptation to the endophytic environment during the switching process. Scanning electron microscopy (SEM) further revealed differences in the cell morphology of the two variants. Specifically, ancestral SA187Y cells were more elongated than SA187W switcher cells (unpaired *t*-test: $p < 0.0001$; Supporting information Figure S2B,C), with an average cell length of $1.44 \pm 0.01\,\mu m$ (mean ± SEM) for SA187Y and $1.31 \pm 0.01\,\mu m$ for SA187W. Using Congo Red staining, we observed that while ancestral SA187Y colonies remained white, SA187W colonies developed a pale pink coloration within 24 h of incubation, indicative of biofilm formation (Supporting information Figure S2D). This phenotype remained stable after a week, indicating that the switcher variant not only differs in morphology but also in its surface-associated behaviours. In addition, SA187W exhibited enhanced sliding motility and radial movement, spreading more extensively across the medium surface than ancestral SA187Y (Supporting information Figure S2E). Comparison of antioxidative capacity revealed that SA187Y possesses higher catalase activity with rapid oxygen production (Supporting Information Figure S2F), further supporting a shift in lifestyle.

3.4 | Metabolic Profiling of the SA187 Ancestor and Switcher Variants

Biolog PM plates were employed to elucidate the differences in metabolic capabilities, nutrient utilisation, and stress responses between the ancestor SA187Y and the white switcher SA187W (Figure 2, Supporting information Figure S3).

3.4.1 | Carbon Utilisation

Carbon metabolism assays using PM1 and PM2 plates revealed that SA187Y and SA187W variants were able to utilise 65 and 77 carbon sources, respectively, out of the 190 tested. (Supporting information Figure S3). All the carbon sources metabolised by SA187Y were also utilised by the switcher SA187W, with the latter showing higher metabolic rates in several cases (Supporting information Figure S3).

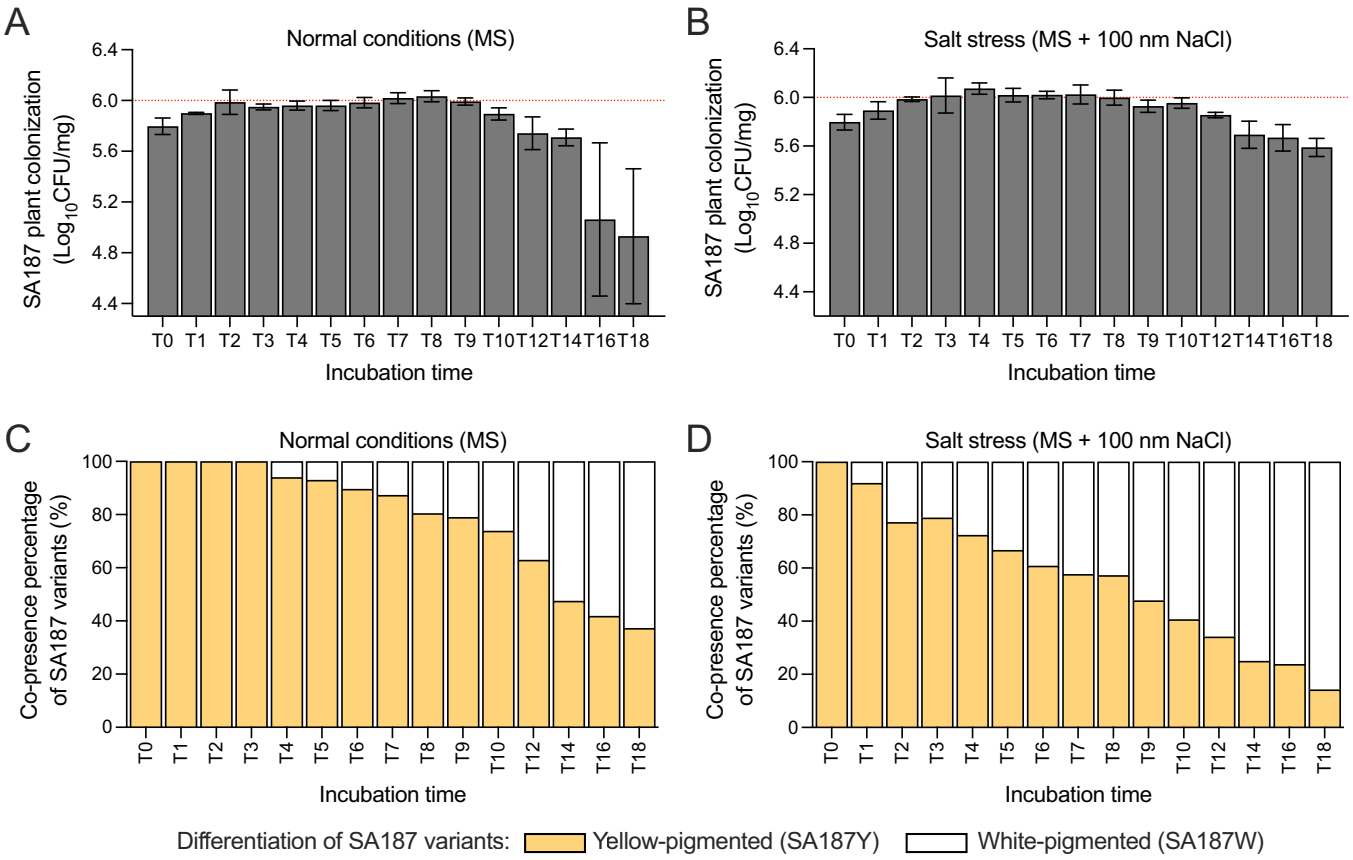

FIGURE 1 | Time series of colonisation of Arabidopsis by SA187Y and the ratio of phenotypic switching of SA187. (A and B) Count of colony-forming units (CFU) of SA187Y per mg of *A. thaliana* grown for 18 days under normal (1/2 MS) and salt stress (1/2 MS + 100 mM NaCl) conditions, respectively. Values are expressed as $\log_{10}$ of CFU/mg values obtained from three independent experiments (see methods). T0 corresponds to 5-day-old SA187 pre-colonised seedlings before transfer to fresh ½ MS or ½ MS + 100 mM NaCl media. The red dotted line indicates 6.0 $\log_{10}$(CFU/g) as a reference. (C and D) From the same plates, the ratio of phenotypic switching (from SA187Y to SA187W) in colonies re-isolated from *A. thaliana* grown was assessed under normal and salt stress conditions, respectively. The number of colonies counted ranged between 35 and 50, depending on the colonies obtained on the LB plates. Values were expressed as the percentage of yellow- and white-pigmented colonies relative to the total number of colonies counted across three independent experiments. [Color figure can be viewed at wileyonlinelibrary.com]

Among the carbon sources metabolised only by switchers, we found pectin, dextrin, arabinose, pyruvic acid, asparagine, and sucrose (Figure 2A–D, Supporting information Figure S3). Such differences in the metabolised carbon sources indicate a potential metabolic divergence between the two strain variants for complex carbohydrates.

3.4.2 | Osmotic/Ionic Response

Salinity and osmolyte sensitivity assays using PM9 plates showed that metabolic activity of both SA187Y and SA187W variants was inhibited by the increasing concentrations of different osmolytes, including sodium chloride, sodium formate, urea, sodium lactate, and sodium benzoate (Supporting information Figure S3). However, in the case of high salinity (8% of NaCl; Figure 2E) and sodium formate (4%, Figure 2F), SA187W remained metabolically active and competitive, likely reflecting its adaptation to osmotic stresses encountered within plant tissues. Notably, the concentrations of the other tested osmolytes (potassium chloride, sodium sulphate, ethylene glycol, sodium phosphate, ammonium sulphate, sodium nitrate, and sodium nitrite) did not affect the metabolism of the two phenotypic variants (Supporting information Figure S3).

3.4.3 | pH Response

Alkaline and acidic environments experienced by free-living bacteria in arid soils and endophytic bacteria colonising the plant apoplast, respectively, are mimed by the reagents present in the PM10 plate. Under acidic conditions (pH 4.5, well A3 and lines B–D), only SA187W maintained an active metabolism, indicating a greater acidity tolerance than ancestral SA187Y (Figure 2G, Supporting information Figure S3). In contrast, both strains showed similar metabolic activities under alkaline conditions (pH 9.5, well A11 and lines E–G) (Figure 2H, Supporting information Figure S3).

These findings highlight notable metabolic differences between the two SA187 variants, particularly in the enhanced capacity of SA187W to utilise a broader range of carbon sources and to tolerate acidic and osmotic stress. These traits may confer a selective advantage during the colonisation of plant tissues.

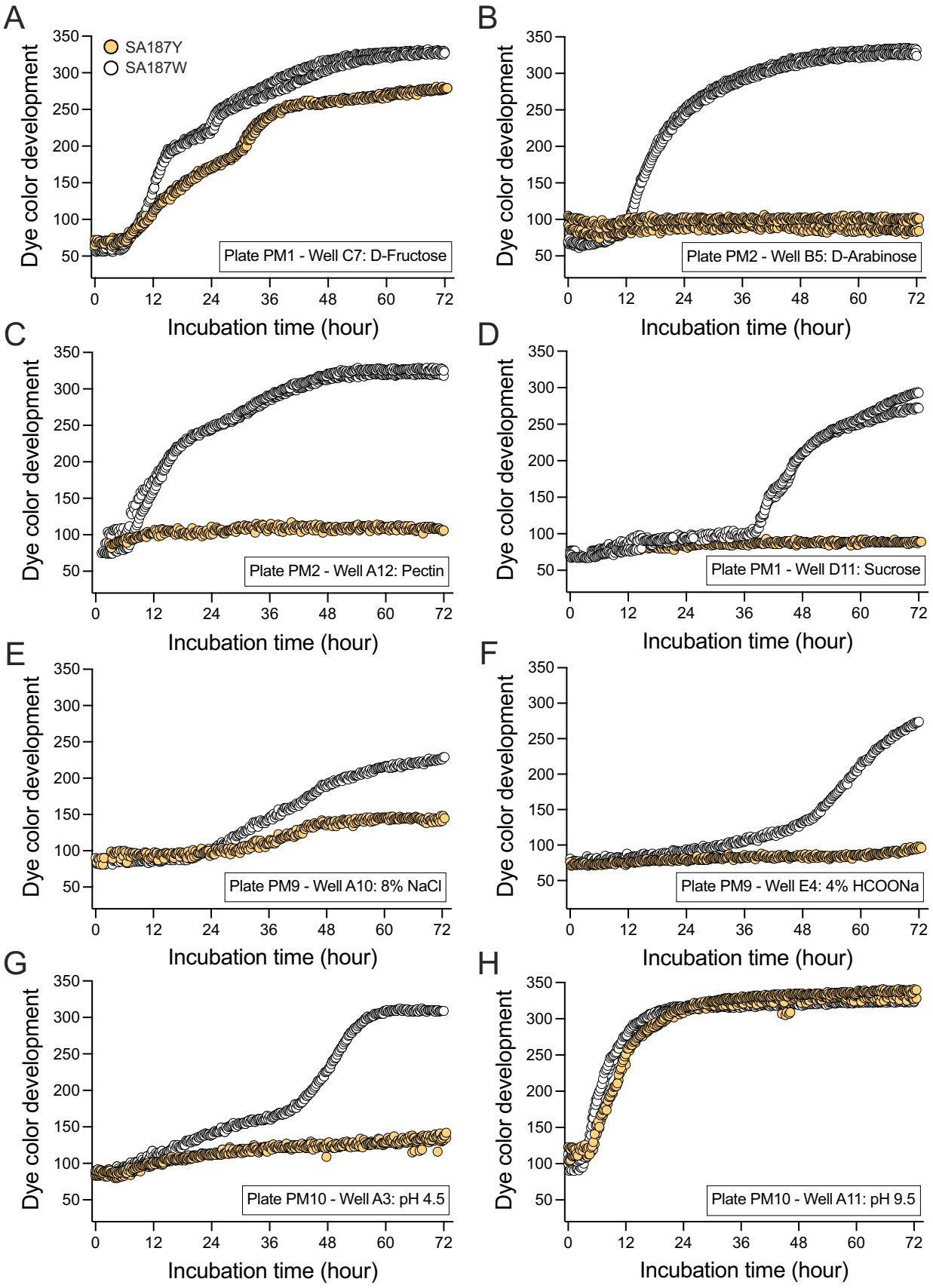

FIGURE 2 | Biolog phenotype of the ancestral and switcher variants of strain SA187. Metabolic activity of SA187W (ancestral) and SA187Y (switcher) in presence of: (A) D-Fructose, (B) D-Arabinose, (C) Pectin and (D) Sucrose as sole carbon sources; (E) 8% sodium chloride (NaCl) and (F) 4% sodium formate (HCOONa) as osmolytes; (G) alkaline and (H) acidic pH conditions (9.5 and 4.5, respectively). The metabolic activity was registered as dye formation every 25 min per well over the entire incubation period of 72 h. For each PM plate, two replicates were done and reported in the graph. [Color figure can be viewed at wileyonlinelibrary.com]

3.5 | Switchers Carry Loss-of-Function Mutations in the RNA Polymerase Sigma Factor S

To determine whether genetic changes underlie the phenotypic switching, we sequenced and compared the genomes of three independent switchers (SA187W1, SA187W2 and SA187W3) along with SA187Y re-isolated from Arabidopsis tissues after 16 days post colonisation. The genomic analysis revealed consistent single nucleotide polymorphisms "SNP" (point mutation, deletion or substitution) that led to frameshifts or a premature stop codon in the gene SA187PBcda_000000191, which encodes the RNA polymerase sigma factor S (RpoS) (Table 1A). To assess the frequency and distribution of *rpo*S mutations within switchers, we additionally analysed 96 yellow and 96 white colonies. After amplification of the *rpo*S gene, we sequenced the *rpoS* gene from 20 colonies, revealing that yellow colonies all retained an intact *rpo*S gene, whereas all switchers exhibited point mutations at various locations within the *rpoS* gene (Table 1B). Notably, while random SNPs were observed in all genomes, mutations in the *rpo*S gene were exclusively found in switcher colonies. Importantly, all deletions and substitutions in the *rpoS* locus of switchers resulted in either a premature stop codon or a frameshift mutation, rendering the mutant versions of the *rpoS* transcriptional regulator nonfunctional (Table 1B).

The frequency of mutations in the *rpo*S gene is significantly higher than random SNPs across the entire genome. With a genome size of 4 429 597 bp (Andrés Barrao et al. 2017), the occurrence of random SNPs occurred at a rate of 2.26×10^{-6} base pairs whereas the *rpoS* gene exhibited an approximately 100-fold higher mutation rate (1.48×10^{-3} base pairs), indicating that phenotypic switching in SA187 is due to selective mutations in the *rpoS* gene and not a general increase in mutation rates in the genome.

3.6 | *rpoS* Gene Disruption Abolishes Carotenoid Production in Switchers

To determine whether the yellow pigmentation of SA187Y results from carotenoid production, which is encoded by the biosynthetic gene cluster (*crt*Eidi-*crt*XYIBZ, SA187PBcda_000002248-000002254), HPLC profiling was performed. The analysis confirmed that SA187Y produces both carotenoids and apocarotenoids, whereas the switcher SA187W variants lack both compounds (Supporting information Figure S4). Notably, this finding was further supported by the lack of expression of the carotenoid biosynthesis genes in switchers compared to ancestral SA187Y (Supporting information Figure S5). Together, these results indicate that the loss of yellow pigmentation during the phenotypic switch is driven by downregulation of the carotenoid biosynthetic pathway.

3.7 | SA187 Tn5-transposon Mutant Library Screening

Since genome comparison of ancestral and white SA187 switchers revealed mutations targeting the *rpoS* gene upon plant-microbe interaction, a whole-genome transposon insertion library was constructed using the EZ-Tn5 transposon system. This method allowed for the random insertion of an EZ-Tn5 transposon into the SA187 genome. White colonies derived from this transposon library were subsequently analysed to assess whether other genes played a role in establishing the white switcher phenotype. Among the 10 white colonies selected, we identified mutations in two genes: *rpoS*, previously detected, and isopentenyl-diphosphate delta-isomerase (*idi*), a key enzyme for carotenoid biosynthesis. The two mutants were designated as SA187Ω*rpoS* and SA187Ω*idi*, respectively. These results showed how mutations in either *rpoS* or *idi* directly cause the loss of yellow pigmentation, leading to the white phenotypes observed in SA187.

3.8 | Gene Regulation in SA187Y and SA187W Variants

RNA-seq was performed to compare the transcript expression levels of the ancestral yellow SA187Y with a naturally occurring SA187W switcher *rpoS* mutant in the logarithmic (6 h) and the stationary phase (18 h). The transcriptome data of SA187Y and SA187W were organised by hierarchical clustering into 12 groups of differentially expressed genes (DEGs) according to their expression patterns that are affected by the logarithmic and the stationary phase. Then, the clusters were analysed for their GO terms and pathway enrichments. Among the 12 obtained clusters, the most divergent and informative clusters were clusters 1, 4, 7, 10,11 and 12 (Figure 3).

Cluster 1 had 50 DEGs that are mainly enriched for sulphur and aspartate amino acid metabolic processes, and the enriched pathways were mainly those of the cysteine and methionine metabolism, the genes exhibited significant downregulation in the wild-type SA187Y during the logarithmic phase (6 h) but significant upregulation during the stationary phase (18 h) (Figure 3). During the logarithmic phase, switcher SA187W showed upregulation of gene expression. However, in the stationary phase, the overall gene expression of the SA187W switcher remained upregulated or was only slightly reduced compared to the logarithmic phase of SA187W (Figure 3).

Cluster 4 had the largest number of DEGs among the twelve clusters, with 332 DEGs that are mainly involved in trehalose metabolic processes. The overall trend of gene expression showed upregulation of these genes in SA187Y in the logarithmic and stationary phases. Interestingly, in the SA187W switcher, the overall gene expression trend showed the opposite trend of a significant downregulation in both logarithmic and stationary phases (Figure 3).

Cluster 7 contained a total of 130 DEGs that exhibited upregulation during the logarithmic phase of SA187Y, followed by a significant downregulation during the stationary phase (Figure 3). In the SA187W switcher, these genes show a slight upregulation in the logarithmic followed by a similar downregulation as in the stationary phase of SA187Y. The genes in this cluster are mostly involved in translation and ribosome biosynthetic processes.

Cluster 10 had 216 DEGs that were mainly involved in the transport of carbohydrates of the starch and sucrose metabolism.

TABLE 1 | Assessment of the mutations in the RNA polymerase sigma factor S (RpoS) in SA187Y and SA187W.

A

SA187	Position	Locus ID	Reference	Alternate	SA187Y	SA187W	SA187W2	SA187W3
	139004	SA187PBcda_000000191	C	A	C	C	A	C
CP019113.1	139210	SA187PBcda_000000191	C	T	C	T	C	C
	139333	SA187PBcda_000000191	CG	C	CG	CG	CG	C

B

SNP position	SA187 reference	SA187 white	SA187 white alternate	SA187 yellow	SA187 yellow alternate
138755	**C**	SA187W-Pool 1	A	SA187Y-Pool 1	**C**
138767	**C**		A		**C**
139133	**C**	SA187W-Pool 2	A	SA187Y-Pool 2	**C**
139245	**A**		AG		**A**
139523	**C**		A		**C**
139133	**C**	SA187W-Pool 3	A	SA187Y-Pool 3	**C**
139523	**C**		A		**C**
138710	**CACGCAGACG**		C		**CACGCAGACG**
138755	**C**	SA187W-Pool 4	A	SA187Y-Pool 4	**C**
139281	**G**		C		**G**
139133	**C**	SA187W-Pool 5	A	SA187Y-Pool 5	**C**
138767	**C**		A		**C**
139133	**C**	SA187W-Pool 6	A	SA187Y-Pool 6	**C**
138755	**C**	SA187W-Pool 7	A	SA187Y-Pool 7	**C**
139281	**G**		C		**G**
138755	**C**	SA187W-Pool 8	A	SA187Y-Pool 8	**C**
139133	**C**		A		**C**
139133	**C**	SA187W-Pool 9	A	SA187Y-Pool 9	**C**
139245	**A**		AG		**A**
139133	**C**	SA187W-Pool 10	A	SA187Y-Pool 10	**C**
136095	**C**		A		**C**
139592	**C**		A		**C**

Note: (A) MiSeq sequencing comparative genomics revealing mutations in the RpoS sigma factor. Comparison of SA187Y, SA187W, SA187W1 and SA187W3 sequences of the *rpoS* gene with reference to the SA187Y genome. (B) Comparative genomics of 100 yellow and white SA187 strains by sequencing 10 pools of 10 strains. Changes in the *rpoS* gene sequence compared to the reference genome of SA187Y are reported.

These genes were significantly downregulated in the logarithmic and stationary phases of SA187Y, whereas they were highly induced in the SA187W switcher in both the logarithmic and stationary phases (Figure 3).

Cluster 11 had a total of 276 DEGs that were downregulated in both the ancestral SA187Y and the SA187W switcher in the logarithmic phase and upregulated in the stationary phases. The GO analysis of these genes revealed their involvement in the hydrolase activity of glycosylated metabolites (Figure 3).

Cluster 12 had 248 DEGs. In this cluster, an interesting expression pattern is related to the growth phase of each strain, with most genes showing enrichment for membrane and ABC transporters. The genes are mainly downregulated in the logarithmic phase of SA187Y and highly induced in the stationary phase, while in the SA187W switcher, they are mainly downregulated in the logarithmic phase with a slight induction in the stationary phase (Figure 3).

Since RpoS is known for having a major role in the transition to the stationary phase regulating (Battesti et al. 2011), the transition from the logarithmic to the stationary phase was also compared for SA187Y and SA187W. For SA187Y, the transition showed significant differential expression of a total of 994 genes, accounting for 24% of the SA187 genome. Among these, GO analysis of the 740 upregulated DEGs revealed that the majority were involved in carbohydrate metabolism and transport, membrane and ABC transporters and localisation (Supporting information Table S1). Some DEGs were enzymes

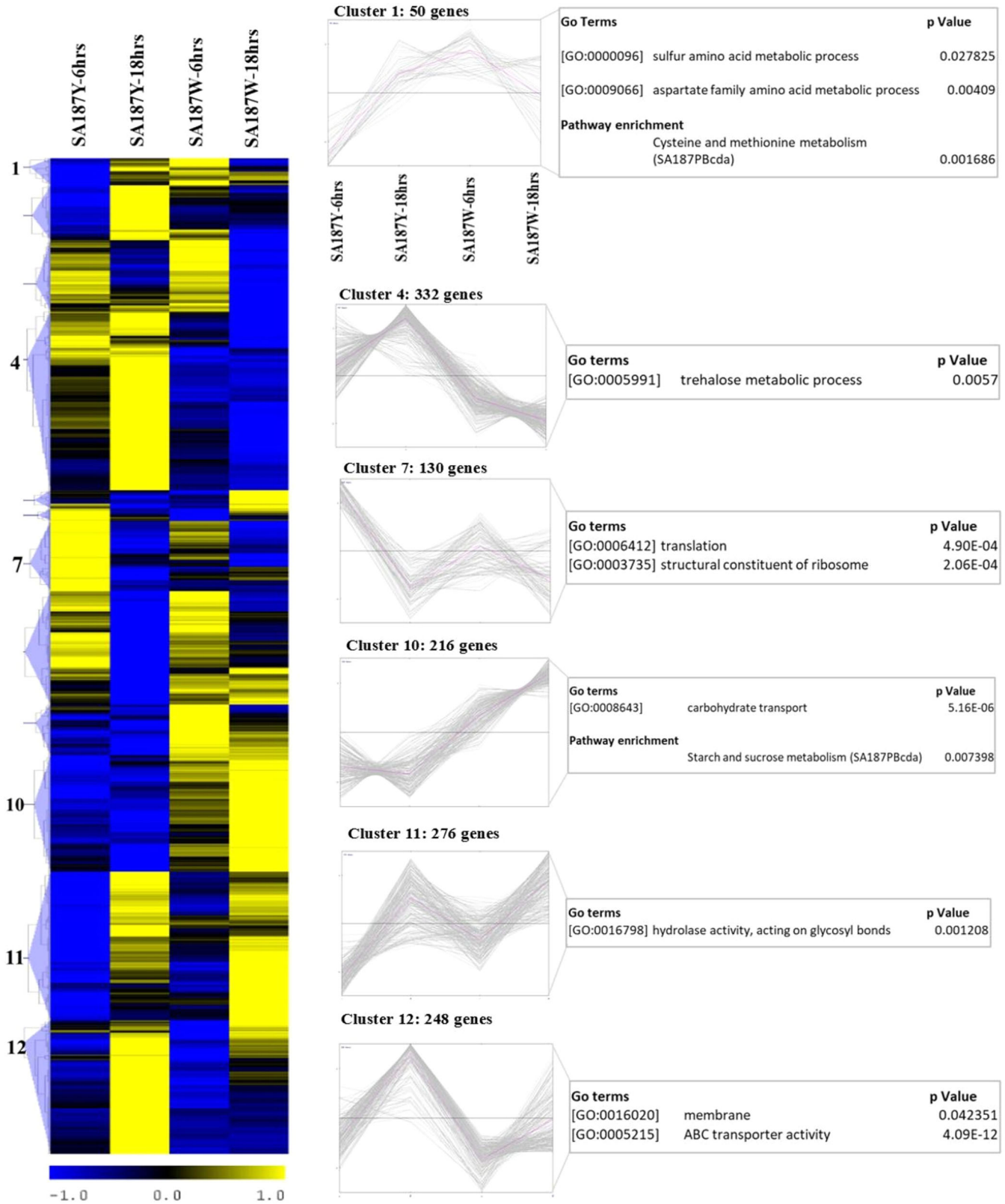

FIGURE 3 | Transcriptome analysis of ancestral and switcher variants of strain SA187. RNA-Seq for SA187Y and SA187W in logarithmic (6 h) and stationary phase (18 h) of bacterial growth. Heatmap of hierarchical clustering, expression profiles of DEGs with GO terms for each cluster. FPKM values of every gene were normalised. Yellow indicates an increase, while blue indicates a decrease in the gene expression level, $p < 0.05$ and a fold change cut-off at log2 > or < of 1.6. The pink line in each cluster shows the general pattern of differentially expressed genes across the two growth conditions for each bacterial strain. [Color figure can be viewed at wileyonlinelibrary.com]

and transporters of several carbohydrate metabolic pathways, such as fructose (*fru*A, PTS system fructose-specific IIC component), mannose (*man*C, mannose-1-phosphate guanylyltransferase), glucose (*glg*C, glucose-1-phosphate adenylyltransferase), and trehalose (*ots*A, trehalose 6-phosphate synthase and *tre*A/*tre*F, alphaalpha-trehalase). Other DEGs were involved in the starch and sucrose metabolism (*glg*X, glycogen operon protein and *glg*Y, alpha-D-glucan 1-alpha-D-glucosylmutase), as well sugar transporters (*set*A, sugar efflux transporter and *araH*, L-arabinose transport system) (Supporting information Table S2). 110 upregulated genes in SA187Y were involved in regulating membrane transport mainly of ABC transporters for several amino acids (*glt*K, glutamate/aspartate ABC transporter permease protein, *sda*A, L-serine dehydratase, and *art*Q, arginine transport system), and minerals including iron (*afu*B/*fbp*B, iron (III) transport system permease protein), zinc (*znuB*, zinc transport system permeases), phosphate (*pstC*, phosphate transport system) and sulphate (*sulP*, sulphate permeases), but also potassium (KdpC, K^+ transporting ATPase), calcium (*cha*A, Ca^{2+} antiporter), hydrogen (H^+ antiporter), and sodium (N^+ symporter) (Supporting information Table S2). Another GO category of DEGs was related to localisation and type II or III secretion systems (e.g., bacterial type II and III secretion system protein IPR004846), flagella (*flh*A flagellar biosynthesis protein FlhA), polyamines transporters (spermidine/putrescine), and pili (*fim*C, *fim*D genes) (Supporting information Table S2). In addition, and confirming the role of RpoS in stress regulation (Battesti et al. 2011), several DEGs were related to stress, such as acid multidrug resistance, and osmoprotectants or the degradation of amino acids, sugars, and fatty acids (Supporting information Table S2). The antioxidative capacity of SA187Y and SA187W was also compared by determining catalase activity. SA187Y exhibited robust catalase activity, evidenced by rapid oxygen production, whereas SA187W showed significantly reduced activity (Supporting information Figure S2).

261 downregulated DEGs in the transition to the stationary phase of SA187Y were involved in cellular biosynthetic processes, such as protein and macromolecule biosynthesis, transcriptional, translational, and gene expression, chemotaxis and two component systems. Several of these DEGs were also involved in nitrogen, as well as purine and pyrimidine metabolism (Supporting information Table S3).

The transcriptome analysis of the transition to the stationary of SA187W revealed a total of 659 DEGs (15% of SA187W genome). Only 200 upregulated DEGs were found and had GO terms of histidine phosphorylation and chromosome condensation, but no significant KEGG pathways were identified (Supporting information Table S4). Most of the SA187W DEGs were downregulated (459 genes) and involved in cellular biosynthesis, protein metabolism, transcriptional, translational and gene expression processes related to ribosome biosynthesis (Supporting information Table S4).

Overall, the transcriptome analysis reveals that SA187Y undergoes major transcriptional changes when transitioning from the logarithmic to the stationary phase. Since these changes do not occur in the SA187W switcher, the regulation of these genes and hence the metabolic reprogramming is dependent on RpoS function. Importantly, RpoS-mediated transcriptional changes appear to support the metabolic adaptation of SA187Y to the host plant apoplast environment.

3.9 | Induction and Reversion of Phenotypic Switching in SA187 Under In Vitro Conditions

To investigate whether cultivation conditions can trigger phenotype switching of SA187 in vitro, we transferred SA187Y colonies from standard LB plates to LB plates supplemented with 20% sucrose to mimic the sucrose-rich conditions of the plant apoplast compartment. While the natural rate of phenotypic switching from yellow- to white-pigmented colonies was very low under standard LB incubation, with only 1.9% of SA187W colonies observed after 72 h of incubation (Supporting information Figure S6A,B), this proportion drastically increased in favour of the white-pigmented SA187W phenotype in the presence of sucrose (Supporting information Figure S6C). However, the colonies obtained showed shiny and slimy morphology, likely due to the high concentration of sucrose present in the growth medium. Since SA187Y and SA187W variants typically appear together, even if in variable ratios depending on growth conditions and incubation time, we sought to determine whether the lab-induced white phenotype can revert back to yellow. Specifically, removing the sucrose stimulus and returning SA187W colonies to standard LB medium resulted in a mixed phenotype with both white-pigments and yellow-pigmented SA187 colonies (Supporting information Figure S6D). Sequence analysis confirmed that the yellow back-switcher colonies, induced by the removal of sucrose, were due to a reverse mutation of the same nucleotide that was mutated in the *rpoS* gene of the original white variant (Supporting information Figure S6E). These results indicate that phenotypic switching in SA187 is a genetically reversible process in adaptation to altered growth conditions.

3.10 | Phenotypic Analysis of Arabidopsis Colonised by Ancestral and Switcher Variants of SA187 Under Normal and Salt Stress Conditions

To assess whether phenotypic switching alters the growth-promoting activity of SA187 (Andrés Barrao et al. 2017), Arabidopsis seeds were inoculated at germination with SA187Y, SA187W, SA187Ω*rpo*S (i.e., white-pigmented mutant generated by mutation of the *rpoS* gene), and SA187Ω*idi* (i.e., white-pigmented mutant generated by mutation of the *idi* gene) strain variants/mutants. Seedlings were exposed to bacterial strains for 5 days before being transferred to either normal or salt-supplemented medium for an additional 16 days. Under normal conditions (½MS, no salt stress), SA187Y was the only variant that significantly promoted plant growth, resulting in a 26% increase in total fresh weight compared to the control (linear mixed model, pairwise comparison: SA187Y vs control, $p < 0.05$) (Figure 4A, Supporting information Table S5). Under salt stress, all SA187 variants increased fresh weight compared to the control, with the strongest effect observed for SA187Y (69%), an intermediate effect for SA187Ω*idi* (57%), and the lower effects for SA187W (38%) and SA187Ω*rpo*S (44%) (Figure 4A, Supporting information Table S5). All SA187 strain variants also increased lateral root density under

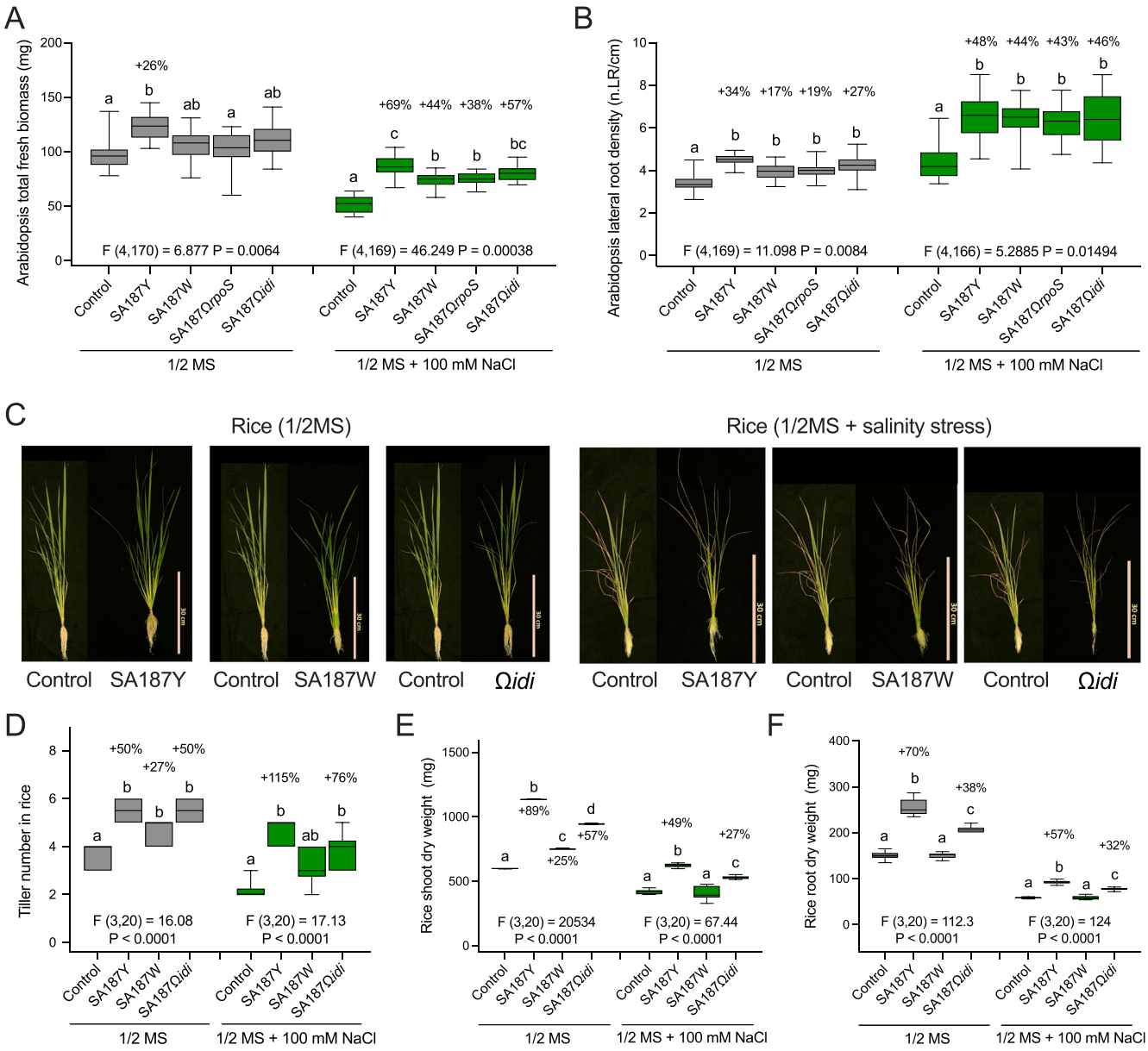

FIGURE 4 | Phenotypic analysis of Arabidopsis and rice colonised by SA187Y, SA187W, SA187Ω*rpoS*, and SA187Ω*idi* under normal and salt stress conditions. (A) Total fresh weight (mg/plant) and (B) lateral root density of *A. thaliana* treated with SA187Y, SA187W, SA187Ω*rpoS* and SA187Ω*idi* mutants under normal and salt stress conditions. Data from three independent experiments, each with two plates of six plants per treatment, are plotted as bar plots. Results of the linear mixed model analysis are shown for each condition; different letters denote statistically significant pairwise differences ($p < 0.05$). The corresponding analysis of variance is reported in Supporting information Table S5. (C) Five-week-old *O. sativa* plants treated with SA187Y, SA187W, and SA187Ω*idi* mutants under normal (left side: ½ MS medium) and salt stress (right side: ½ MS + 100 mM NaCl) conditions. The bars indicate 30 cm scale. (D) Number of tillers, (E) shoot dry weight (mg per plant, $n = 6$), and (F) root dry weight (mg per plant, $n = 6$) of rice 5-week-old plants. Values represent the means of six plants grown in the same hydroponic container; error bars indicate standard error. One-way ANOVA and pairwise comparisons are reported, with different letters indicating statistically significant differences (Turkey's test, $p < 0.05$). [Color figure can be viewed at wileyonlinelibrary.com]

both normal and salt stress conditions, with no significant differences among them in the extent of this effect (Figure 4B, Supporting information Table S5).

These results demonstrate that mutations in the *rpoS* gene—whether naturally occurring in SA187W or engineered in SA187Ω*rpoS*—substantially impair the growth-promoting effects of SA187 in Arabidopsis, under both normal and salt stress conditions.

3.11 | Phenotypic Analysis of *Oryza sativa* Colonised by Ancestral and Switcher Variants of SA187 Under Normal and Salt Stress Conditions

Since the SA187W switchers showed reduced beneficial effects on Arabidopsis growth and development, we next investigated whether such reduction was host-specific. Rice seedlings were inoculated with SA187Y, SA187W, and the white-pigmented mutant SA187Ω*idi* for a 5-week period (Figure 4C). Under

normal conditions, both SA187Y and SA187Ω*idi* significantly increased tiller number to a comparable extent, whereas SA187W treatment conferred only a modest improvement (Figure 4D). Similarly, under salt stress, SA187Y and SA187Ω*idi* exerted a significant beneficial effect, while SA187W did not (Figure 4D). Assessment of shoot dry biomass under normal conditions further confirmed the observed promotion pattern, but in this case, defining a clear ranking of promotion with 89% increase mediated by SA187Y, 57% by SA187Ω*idi*, and only 25% by SA187W (Figure 4E). Despite an overall reduction in plant biomass caused by salt stress, the growth-promotion pattern mediated by SA187 variants remained largely consistent, with the notable exception of SA187W, which failed to confer any measurable beneficial effect under these conditions (Figure 4E). The differential effects of the SA187 variants on total biomass were also mirrored in the root biomass (dry weight) measurements under both normal and salt stress. Only SA187Y and SA187Ω*idi* significantly promoted root dry weight, with SA187Y displaying the strongest effect (Figure 4F). Notably, SA187W had lost all promoting effects, and such a lack of benefit on the root system was evident even under normal growth conditions (½ MS, Figure 4F).

These results demonstrate that phenotypic switching in SA187 induced by mutations in the *rpoS* gene (as represented by SA187W) markedly compromises the strain's ability to promote rice growth under both normal and salt stress conditions. In comparison, white-switch phenotypes originated by disruption of the carotenoid biosynthetic pathway (here as SA187Ωidi) resulted in only a moderate reduction in plant growth promotion (i.e., dry biomass), suggesting that carotenoid production may not play a central role in SA187's plant-beneficial activity. This distinction highlights *rpoS*-mediated regulatory shifts as key determinants of endophytic performance and stress resilience.

4 | Discussion

Enterobacter sp SA187 is a facultative endophytic bacterium with multi-abiotic-stress-promoting activity under laboratory and field conditions on several plant species (de Zélicourt et al. 2018; Saad et al. 2020; Shekhawat et al. 2021). SA187 primarily forms yellow colonies when growing on LB (SA187Y). In rare cases, white colonies can be found in culture from LB medium upon the stationary phase (Supporting information Figure S6A), suggesting that phenotypic switching is a rare random event under standard laboratory conditions. However, upon plant colonisation, such a phenotypic switch from the ancestral yellow (SA187Y) to white (SA187W) colonies was favoured, and SA187W became the dominant variant in the population, particularly under stress conditions such as salinity. These findings suggest that plant-associated environments—and especially environmental stresses—act as selective pressures driving phenotypic switching and adaptation within SA187 populations.

The shift from yellow to white pigmentation correlates with a downregulation of carotenoid biosynthesis, driven by consistent point mutations in the RNA polymerase sigma factor S (*rpoS*) gene. RpoS is a transcriptional regulator for RNA polymerase, functioning as a global stress regulator in bacteria, including oxidative stress defence, stationary phase adaptation, and secondary metabolism, which includes carotenoid production. RpoS also controls resistance to DNA damage, osmotic shock, oxidative stress, acidity, and biofilm formation (Battesti et al. 2011; Corona-Izquierdo and Membrillo-Hernã¡ndez 2002; Ito et al. 2008; Johler et al. 2010; Merrikh et al. 2009; Vijayakumar et al. 2004). The occurrence of premature stop codons and frameshift mutations in *rpoS* (Battesti et al. 2011) aligns with previous observations linking these mutations to adaptation under nutrient limitation (Finkel 2006; Martínez-García et al. 2003). Strikingly, in the SA187 population, *rpo*S mutations appeared to be positively selected during plant colonisation, showing a several hundred-fold higher mutation rate in the gene than in the free-living state, at far higher frequencies than observed in free-living states. This suggests that the endophytic environment exerts selective pressures favouring the emergence of SA187W variants.

Since the phenotypic switch occurs in various plant hosts, the selective advantage of SA187W appears to be linked to the conditions predominating in the endophytic state in the plant host. Such findings fit into broader concepts of microbial adaptation: phenotypic plasticity and regulatory rewiring allow bacteria to rapidly adjust to fluctuating environments. Regulatory circuits like RpoS play a pivotal role in mediating this plasticity, providing flexibility in response to the complex and variable conditions encountered within plant tissues. These observations align with established theories positing that fluctuating environments favour regulatory mechanisms that enable rapid phenotypic shifts crucial not only for immediate survival but also for the evolutionary processes of bacterial populations (Spratt and Lane 2022). Moreover, SA187W exhibits distinct physiological traits compared to its ancestral form. Reduced growth rates, smaller cell size, enhanced motility, and increased biofilm formation mirror phenotypes reported for RpoS mutants in other bacteria such as *Escherichia coli*, *Pseudomonas fluorescens* and *Serratia marcescens* (Corona-Izquierdo and Membrillo-Hernã¡ndez 2002; Liu et al. 2019). For instance, enhanced motility (Qin et al. 2020) and biofilm formation, such as found in *Pseudomonas* (Li, de Jonge, et al. 2021; Li, Zhang, et al. 2021) and *Bacillus* (Lin et al. 2021; Nordgaard et al. 2022), may reflect beneficial adaptations within the unique environments of plant tissues, where dispersal and niche occupation are advantageous. Similarly, reduced catalase activity in SA187W suggests that reactive oxygen species (ROS) defences, critical in rhizosphere life, may be dispensable within the protected apoplastic environment of host tissues (Apel and Hirt 2004). These physiological changes represent a trade-off, where fitness advantages in the plant interior come at the cost of reduced competitiveness in free-living, nutrient-rich environments. The diminished PGP activity of SA187W in Arabidopsis and rice under both normal and salt stress conditions indeed underscores the functional implications of these phenotypic switches. While RpoS mutations may confer fitness advantages within the plant endosphere, they appear detrimental to the bacterium's ability to promote plant growth under broader environmental conditions. This is because mutations in a bacterial population can give rise to reduced fitness under given conditions, but the phenotypes may become advantageous under altered environmental conditions.

Interestingly, phenotypic switching of white variants in SA187 is not necessarily irreversible. Under laboratory conditions,

reversion of white to yellow SA187 variants was observed, and this process was strongly enhanced by high sucrose conditions. Moreover, we could show that the mutated nucleotide in the *rpoS* gene that was responsible for the white SA187 phenotype could revert to its wild-type yellow form, showing that phenotypic switching is a purely genetic process. This phenomenon aligns with broader observations in microbiology, where phenotypic plasticity and reversible switching serve as crucial survival strategies in fluctuating environments. Reversible switching in bacteria has been widely reported as a bet-hedging strategy that allows populations to survive sudden environmental shifts by maintaining subpopulations in distinct physiological states (Morawska et al. 2022). In fact, in the SA187 population, phenotypic switching and the resulting mixing of ancestors and switchers contribute to its ecological flexibility and success as both a soil inhabitant and a facultative endophyte. It represents a strategy for optimising fitness across contrasting environmental niches: in soil or rhizosphere-like environments, the yellow-pigmented, stress-resistant ancestral form (*rpoS*-intact) is better adapted to withstand fluctuating abiotic stresses, whereas within the relatively stable environment of the plant apoplast, the white-pigmented switcher (*rpoS*-mutated) possesses traits that favour tissue colonisation, biofilm formation, metabolic competition, and stress tolerance.

5 | Conclusion

The *rpoS* mutations identified in SA187 phenotypic switchers highlight a sophisticated adaptation mechanism, where the bacterium shifts its phenotypic and metabolic strategy to adapt from a free-living soil to an endophytic plant environment. The phenotypic heterogeneity arises through random genetic changes in isogenic populations. Although SA187W switching is genetically determined by *rpoS* loss-of-function mutations, reverse mutations can occasionally restore the ancestral state when environmental conditions revert. These findings underscore that rare genetic variants within a bacterial population can be subject to natural selection, depending on environmental pressures that favour specific metabolic programs. This adaptive flexibility plays a crucial role in the successful establishment of symbiotic plant–microbe interactions in vivo.

Acknowledgements

This study was supported by KAUST grant BAS/1/1062-01-01 to H.H. D.D. acknowledges the support of KAUST for the Biolog system analysis through the baseline funding.

Conflicts of Interest

The authors declare no conflicts of interest.

Data Availability Statement

The data that support the findings of this study are openly available in GEO NCBI at https://www.ncbi.nlm.nih.gov/search/all/?term=GSE277260, reference number GSE277260.

References

Andrés Barrao, C., F. F. Lafi, I. Alam, et al. 2017. "Complete Genome Sequence Analysis of Enterobacter sp. SA187, a Plant Multi-Stress Tolerance Promoting Endophytic Bacterium." *Frontiers in Microbiology* 8: 2023. https://doi.org/10.3389/fmicb.2017.02023.

Andrés-Barrao, C., H. Alzubaidy, R. Jalal, et al. 2021. "Coordinated Bacterial and Plant Sulfur Metabolism in *Enterobacter* sp. SA187 Induced Plant Salt Stress Tolerance." *Proceedings of the National Academy of Sciences* 118, no. 46: e2107417118. https://doi.org/10.1073/pnas.2107417118.

Ankati, S., and A. R. Podile. 2019. "Metabolites in the Root Exudates of Groundnut Change During Interaction With Plant Growth Promoting Rhizobacteria in a Strain-Specific Manner." *Journal of Plant Physiology* 243: 153057. https://doi.org/10.1016/j.jplph.2019.153057.

Apel, K., and H. Hirt. 2004. "Reactive Oxygen Species: Metabolism, Oxidative Stress, and Signal Transduction." *Annual Review of Plant Biology* 55: 373–399. https://doi.org/10.1146/annurev.arplant.55.031903.141701.

Bais, H. P., T. L. Weir, L. G. Perry, S. Gilroy, and J. M. Vivanco. 2006. "The Role of Root Exudates in Rhizosphere Interactions With Plants and Other Organisms." *Annual Review of Plant Biology* 57: 233–266. https://doi.org/10.1146/annurev.arplant.57.032905.105159.

Battesti, A., N. Majdalani, and S. Gottesman. 2011. "The RpoS-Mediated General Stress Response in *Escherichia coli*." *Annual Review of Microbiology* 65: 189–213. https://doi.org/10.1146/annurev-micro-090110-102946.

Berg, G., and K. Smalla. 2009. "Plant Species and Soil Type Cooperatively Shape the Structure and Function of Microbial Communities in the Rhizosphere." *FEMS Microbiology Ecology* 68, no. 1: 1–13. https://doi.org/10.1111/j.1574-6941.2009.00654.x.

Bisseling, T., J. L. Dangl, and P. Schulze-Lefert. 2009. "Next-Generation Communication." *Science* 324, no. 5928: 691. https://doi.org/10.1126/science.1174404.

Bolger, A. M., M. Lohse, and B. Usadel. 2014. "Trimmomatic: A Flexible Trimmer for Illumina Sequence Data." *Bioinformatics* 30, no. 15: 2114–2120. https://doi.org/10.1093/bioinformatics/btu170.

Corona-Izquierdo, F. P., and J. Membrillo-Hernã¡ndez. 2002. "A Mutation in Rpos Enhances Biofilm Formation in *Escherichia coli* During Exponential Phase of Growth." *FEMS Microbiology Letters* 211, no. 1: 105–110. https://doi.org/10.1111/j.1574-6968.2002.tb11210.x.

Crombach, A., and P. Hogeweg. 2008. "Evolution of Evolvability in Gene Regulatory Networks." *PLoS Computational Biology* 4, no. 7: e1000112. https://doi.org/10.1371/journal.pcbi.1000112.

Drogue, B., H. Doré, S. Borland, F. Wisniewski-Dyé, and C. Prigent-Combaret. 2012. "Which Specificity in Cooperation Between Phytostimulating Rhizobacteria and Plants?" *Research in Microbiology* 163, no. 8: 500–510. https://doi.org/10.1016/j.resmic.2012.08.006.

Eida, A. A., M. Ziegler, F. F. Lafi, et al. 2018. "Desert Plant Bacteria Reveal Host Influence and Beneficial Plant Growth Properties." *PLoS One* 13, no. 12: e0208223. https://doi.org/10.1371/journal.pone.0208223.

Finkel, S. E. 2006. "Long-Term Survival During Stationary Phase: Evolution and the GASP Phenotype." *Nature Reviews Microbiology* 4, no. 2: 113–120. https://doi.org/10.1038/nrmicro1340.

Haichar, F. Z., C. Marol, O. Berge, et al. 2008. "Plant Host Habitat and Root Exudates Shape Soil Bacterial Community Structure." *ISME Journal* 2, no. 12: 1221–1230. https://doi.org/10.1038/ismej.2008.80.

Haichar, F. Z., C. Santaella, T. Heulin, and W. Achouak. 2014. "Root Exudates Mediated Interactions Belowground." *Soil Biology and Biochemistry* 77: 69–80. https://doi.org/10.1016/j.soilbio.2014.06.017.

Hardoim, P. R., L. S. van Overbeek, G. Berg, et al. 2015. "The Hidden World Within Plants: Ecological and Evolutionary Considerations for Defining Functioning of Microbial Endophytes." *Microbiology and Molecular Biology Reviews* 79, no. 3: 293–320. https://doi.org/10.1128/mmbr.00050-14.

Henderson, I. R., P. Owen, and J. P. Nataro. 1999. "Molecular Switches-The ON and OFF of Bacterial Phase Variation." *Molecular Microbiology* 33, no. 5: 919–932. https://doi.org/10.1046/j.1365-2958.1999.01555.x.

Hirt, H. 2020. "Healthy Soils for Healthy Plants for Healthy Humans: How Beneficial Microbes in the Soil, Food and Gut are Interconnected and How Agriculture Can Contribute to Human Health." *EMBO Reports* 21, no. 8: e51069. https://doi.org/10.15252/embr.202051069.

Ito, A., T. May, K. Kawata, and S. Okabe. 2008. "Significance of RpoS During Maturation of *Escherichia coli* Biofilms." *Biotechnology and Bioengineering* 99, no. 6: 1462–1471. https://doi.org/10.1002/bit.21695.

Johler, S., R. Stephan, I. Hartmann, K. A. Kuehner, and A. Lehner. 2010. "Genes Involved in Yellow Pigmentation of Cronobacter Sakazakii ES5 and Influence of Pigmentation on Persistence and Growth Under Environmental Stress." *Applied and Environmental Microbiology* 76, no. 4: 1053–1061. https://doi.org/10.1128/aem.01420-09.

Krell, T., J. Lacal, A. Busch, H. Silva-Jiménez, M. E. Guazzaroni, and J. L. Ramos. 2010. "Bacterial Sensor Kinases: Diversity in the Recognition of Environmental Signals." *Annual Review of Microbiology* 64: 539–559. https://doi.org/10.1146/annurev.micro.112408.134054.

Li, H., B. Handsaker, A. Wysoker, et al. 2009. "The Sequence Alignment/Map format and SAMtools." *Bioinformatics* 25: 2078–2079.

Li, H., and R. Durbin. 2010. "Fast and Accurate Long-Read Alignment With Burrows-Wheeler Transform." *Bioinformatics* 26, no. 5: 589–595. https://doi.org/10.1093/bioinformatics/btp698.

Li, E., R. de Jonge, C. Liu, et al. 2021. "Rapid Evolution of Bacterial Mutualism in the Plant Rhizosphere." *Nature Communications* 12, no. 1: 3829. https://doi.org/10.1038/s41467-021-24005-y.

Li, E., H. Zhang, H. Jiang, et al. 2021. "Experimental-Evolution-Driven Identification of Arabidopsis Rhizosphere Competence Genes in Pseudomonas Protegens." *mBio* 12, no. 3: e0092721. https://doi.org/10.1128/mBio.00927-21.

Lin, Y., M. Alstrup, J. K. Y. Pang, et al. 2021. "Adaptation of Bacillus Thuringiensis to Plant Colonization Affects Differentiation and Toxicity." *mSystems* 6, no. 5: e0086421. https://doi.org/10.1128/mSystems.00864-21.

Liu, H., L. C. Carvalhais, M. Crawford, et al. 2017. "Inner Plant Values: Diversity, Colonization and Benefits From Endophytic Bacteria." *Frontiers in Microbiology* 8. https://doi.org/10.3389/fmicb.2017.02552.

Liu, X., J. Xu, J. Zhu, P. Du, and A. Sun. 2019. "Combined Transcriptome and Proteome Analysis of RpoS Regulon Reveals its Role in Spoilage Potential of *Pseudomonas fluorescens*." *Frontiers in Microbiology* 10. https://doi.org/10.3389/fmicb.2019.00094.

Marasco, R., M. Fusi, M. Mosqueira, et al. 2022. "Rhizosheath–Root System Changes Exopolysaccharide Content but Stabilizes Bacterial Community Across Contrasting Seasons in a Desert Environment." *Environmental Microbiome* 17, no. 1: 14. https://doi.org/10.1186/s40793-022-00407-3.

Martínez-García, E., A. Tormo, and J. Navarro-Lloréns. 2003. "GASP Phenotype: Presence in Enterobacteria and Independence of σS in its Acquisition." *FEMS Microbiology Letters* 225, no. 2: 201–206. https://doi.org/10.1016/s0378-1097(03)00514-7.

Massalha, H., E. Korenblum, D. Tholl, and A. Aharoni. 2017. "Small Molecules Below-Ground: The Role of Specialized Metabolites in the Rhizosphere." *Plant Journal* 90, no. 4: 788–807. https://doi.org/10.1111/tpj.13543.

McKenna, A., M. Hanna, E. Banks, et al. 2010. "The Genome Analysis Toolkit: A Map Reduce Framework for Analyzing Next-Generation DNA Sequencing Data." *Genome Research* 20, no. 9: 1297–1303. https://doi.org/10.1101/gr.107524.110.

Merrikh, H., A. E. Ferrazzoli, A. Bougdour, A. Olivier-Mason, and S. T. Lovett. 2009. "A DNA Damage Response in *Escherichia coli* Involving the Alternative Sigma Factor, RpoS." *Proceedings of the National Academy of Sciences* 106, no. 2: 611–616. https://doi.org/10.1073/pnas.0803665106.

Mi, J., K. P. Jia, J. Y. Wang, and S. Al-Babili. 2018. "A Rapid LC-MS Method for Qualitative and Quantitative Profiling of Plant Apocarotenoids." *Analytica Chimica Acta* 1035: 87–95.

Morawska, L. P., J. A. Hernandez-Valdes, and O. P. Kuipers. 2022. "Diversity of Bet-Hedging Strategies in Microbial Communities-Recent Cases and Insights." *WIREs Mechanisms of Disease* 14, no. 2: e1544. https://doi.org/10.1002/wsbm.1544.

Nordgaard, M., C. Blake, G. Maróti, et al. 2022. "Experimental Evolution of *Bacillus subtilis* on *Arabidopsis thaliana* Roots Reveals Fast Adaptation and Improved Root Colonization." *iScience* 25, no. 6: 104406. https://doi.org/10.1016/j.isci.2022.104406.

Philippot, L., C. Chenu, A. Kappler, M. C. Rillig, and N. Fierer. 2024. "The Interplay Between Microbial Communities and Soil Properties." *Nature Reviews Microbiology* 22, no. 4: 226–239. https://doi.org/10.1038/s41579-023-00980-5.

Qin, H., Y. Liu, X. Cao, et al. 2020. "Rpos Is a Pleiotropic Regulator of Motility, Biofilm Formation, Exoenzymes, Siderophore and Prodigiosin Production, and Trade-Off During Prolonged Stationary Phase in Serratia Marcescens." *PLoS One* 15, no. 6: e0232549. https://doi.org/10.1371/journal.pone.0232549.

Reinhold-Hurek, B., W. Bünger, C. S. Burbano, M. Sabale, and T. Hurek. 2015. "Roots Shaping Their Microbiome: Global Hotspots for Microbial Activity." *Annual Review of Phytopathology* 53: 403–424. https://doi.org/10.1146/annurev-phyto-082712-102342.

Rudrappa, T., K. J. Czymmek, P. W. Paré, and H. P. Bais. 2008. "Root-Secreted Malic Acid Recruits Beneficial Soil Bacteria." *Plant Physiology* 148, no. 3: 1547–1556. https://doi.org/10.1104/pp.108.127613.

Saad, M. M., A. A. Eida, and H. Hirt. 2020. "Tailoring Plant-Associated Microbial Inoculants in Agriculture: A Roadmap for Successful Application." *Journal of Experimental Botany* 71, no. 13: 3878–3901. https://doi.org/10.1093/jxb/eraa111.

Shekhawat, K., M. M. Saad, A. Sheikh, et al. 2021. "Root Endophyte Induced Plant Thermotolerance by Constitutive Chromatin Modification at Heat Stress Memory Gene Loci." *EMBO Reports* 22, no. 3: e51049. https://doi.org/10.15252/embr.202051049.

Shekhawat, K., A. Veluchamy, A. Fatima, et al. 2024. "Microbe-Induced Coordination of Plant Iron-Sulfur Metabolism Enhances High-Light-Stress Tolerance of Arabidopsis." *Plant Communications* 5: 101012. https://doi.org/10.1016/j.xplc.2024.101012.

Spratt, M. R., and K. Lane. 2022. "Navigating Environmental Transitions: The Role of Phenotypic Variation in Bacterial Responses." *mBio* 13, no. 6: e0221222. https://doi.org/10.1128/mbio.02212-2.

Synek, L., A. Rawat, F. L'Haridon, L. Weisskopf, M. M. Saad, and H. Hirt. 2021. "Multiple Strategies of Plant Colonization by Beneficial Endophytic Enterobacter sp. SA187." *Environmental Microbiology* 23, no. 10: 6223–6240. https://doi.org/10.1111/1462-2920.15747.

Thrash, A., M. Arick, and D. G. Peterson. 2018. "Quack: A Quality Assurance Tool for High Throughput Sequence Data." *Analytical Biochemistry* 548. https://doi.org/10.1016/j.ab.2018.01.028.

Trapnell, C., B. A. Williams, G. Pertea, et al. 2010. "Transcript Assembly and Quantification by RNA-Seq Reveals Unannotated Transcripts and Isoform Switching During Cell Differentiation." *Nature Biotechnology* 28, no. 5: 511–515. https://do.org/10.1038/nbt.1621.

Vijayakumar, S. R. V., M. G. Kirchhof, C. L. Patten, and H. E. Schellhorn. 2004. "RpoS-Regulated Genes of *Escherichia coli* Identified by Random LacZ Fusion Mutagenesis." *Journal of Bacteriology* 186, no. 24: 8499–8507. https://doi.org/10.1128/jb.186.24.8499-8507.2004.

Wheatley, R. M., and P. S. Poole. 2018. "Mechanisms of Bacterial Attachment to Roots." *FEMS Microbiology Reviews* 42, no. 4: 448–461. https://doi.org/10.1093/femsre/fuy014.

van der Woude, M. W., and A. J. Bäumler. 2004. "Phase and Antigenic Variation in Bacteria." *Clinical Microbiology Reviews* 17, no. 3: 581–611. https://doi.org/10.1128/cmr.17.3.581-611.2004.

Yuan, J., J. Zhao, T. Wen, et al. 2018. "Root Exudates Drive the Soil-Borne Legacy of Aboveground Pathogen Infection." *Microbiome* 6, no. 1: 156. https://doi.org/10.1186/s40168-018-0537-x.

de Zélicourt, A., L. Synek, M. M. Saad, et al. 2018. "Ethylene Induced Plant Stress Tolerance by Enterobacter sp. SA187 Is Mediated by 2-keto-4-methylthiobutyric Acid Production." *PLoS Genetics* 14, no. 3: e1007273. https://doi.org/10.1371/journal.pgen.1007273.

Supporting Information

Additional supporting information can be found online in the Supporting Information section.

Supporting Figure S1: Re-isolation of SA187 following colonization of different plant hosts. **Supporting Figure S2:** Biochemical properties of SA187Y and SA187W. **Supporting Figure S3:** Biolog phenotype microarray results of SA187Y and SA187W variants. **Supporting Figure S4:** β-carotene quantification. **Supporting Figure S5:** Gene expression analysis of bacterial carotenoid biosynthesis genes. **Supporting Figure S6:** Assessment of SA187Y and SA187W growth properties. **Supporting Table S1:** Upregulated and downregulated GO terms and enriched pathways for SA187Y in the stationary phase (18 hours) vs logarithmic phase (6 hours). Gene ID corresponds to the SA187 genome in the INDIGO database. p-values were adjusted using the Benjamini and Hochberg approach. **Supporting Table S2:** List of selected upregulated DEGs in SA187Y in stationary (18 hours) vs logarithmic phase (6 hours). Gene ID corresponds to the SA187 genome in the INDIGO database, and $p < 0.05$. *p*-values were adjusted using the Benjamini and Hochberg approach. **Supporting Table S3:** List of selected downregulated DEGs in SA187Y in stationary (18 hours) vs logarithmic phase (6 hours). Gene IDs correspond to the SA187 genome annotated by the INDIGO database, $p < 0.05$. *p*-values were adjusted using the Benjamini and Hochberg approach. **Supporting Table S4:** Upregulated and downregulated GO terms and enriched pathways for SA187W in the stationary phase (18 hours) vs. logarithmic phase (6 hours). Gene ID corresponds to the SA187 genome in the INDIGO database. *p*-values were adjusted using the Benjamini and Hochberg approach. **Supporting Table 5:** Variance components for random effects estimated by the linear mixed-effects model of (variable ~ Treatment + [1|Experiment] + [1|Plate]). Shown are the variance (% of total variance) and standard deviation (SD) for each random effect (Experiment, Plate) and the residual term.